Article published online: 2024-05-31

THIEME OPEN ACCESS

Modification and Structure–Activity Relationship Study of Cyclodepsipeptide Trichodestruxin D Derivatives as Potential Antitumor Agents

Jihua Zou[1#] Yifei Lu[1#] Xiang Li[2] Conghao Gai[2] Yan Zou[2*] Qingjie Zhao[1,2*]

[1] College of Pharmacy, Fujian University of Traditional Chinese Medicine, Fuzhou, People's Republic of China
[2] Department of Organic Chemistry, College of Pharmacy, Naval Medical University, Shanghai, People's Republic of China

Pharmaceut Fronts

Address for correspondence Yan Zou, PhD, College of Pharmacy, Naval Medical University, 800 Xiangyin Road, Shanghai 200433, People's Republic of China (e-mail: zouyan@smmu.edu.cn).

Qingjie Zhao, PhD, College of Pharmacy, Naval Medical University, 800 Xiangyin Road, Shanghai 200433, People's Republic of China (e-mail: qjzhao@smmu.edu.cn).

Abstract

Trichodestruxins A–D are cyclic peptides isolated from the plant endophyte fungus *Trichoderma harzianum* with inhibitory activities against the proliferation of tumor cells. This study aimed to modify the structure of trichodestruxin D (**TD-**(*R*)) to improve its antitumor activity and analyze the structure–activity relationship (SAR) to provide references for lead optimization. In this study, seven **TD-**(*R*) derivatives (**TD-**(*S*), **TD-1**, **2**, **3**, **4**, **5**, **6**) were designed by different strategies, namely amino acid mutation, configuration switching, replacement of ester with amide, and *N*-methylation/demethylation. Those derivatives were prepared by a solid-phase peptide synthesis strategy, and structurally characterized by high-resolution mass spectra. The inhibitory activities of the peptides against the lung carcinoma A549 cells were assessed by determining cellular proliferation and migration using CCK-8 and a 24-well migration plate. Our data confirmed the inhibitory effect of those derivatives on A549 cell proliferation, among which **TD-**(*S*), **TD-1**, and **TD-2** displayed higher inhibitory activity compared with the control (DMSO) group, but their inhibitory activity was slightly decreased than that of **TD-**(*R*). The inhibitory activity of **TD-3**, **TD-4**, and **TD-6** on A549 cell migration was much better than that of **TD-**(*R*). SAR studies demonstrated a pivotal role in the configuration of the residue of 2-hydroxy-4-methyl-pentenoic acid and some residues in the structure of **TD-**(*R*). In conclusion, **TD-3**, **TD-4**, and **TD-6** may be potential agents for the treatment of cancer migration, and our modification methods will provide a reference for the development of anticancer drugs in the future.

Keywords
- cyclodepsipeptides
- cyclic peptide
- cell migration

Introduction

Peptides from natural products with broad biological activities provide opportunities for drug discovery.[1–5] For example, the soybean-derived peptide Vglycin, isolated from soybean seeds, is effective in inhibiting the proliferation of colon cancer cells *in vitro* and *in vivo*.[6] The cecropin XJ, isolated from the larvae of the silkworm *Bombyx mori*, can inhibit the proliferation of cancer cells through the mitochondrial apoptotic pathway, which in turn leads to apoptosis of cancer cells.[1] The peptide (Ala-Trp-Lys-Leus-Leu-Phe-Asp-Asp-Gly-Val), which is extracted from

* *These authors contributed equally to this work.*

received
November 15, 2023
accepted
May 8, 2024

DOI https://doi.org/10.1055/s-0044-1787282.
ISSN 2628-5088.

Georg Thieme Verlag KG, Rüdigerstraße 14, 70469 Stuttgart, Germany

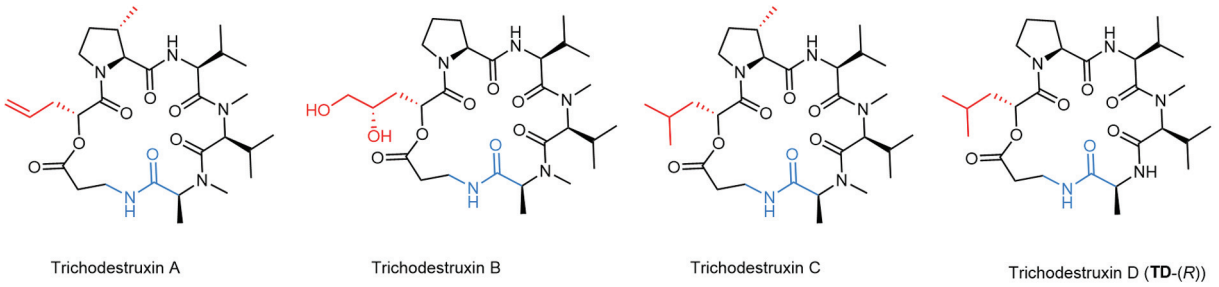

Fig. 1 Structures of trichodestruxin A–D.

palm fern seeds (*Cycas revoluta*), significantly inhibits the proliferation of human epidermoid carcinoma (Hep2) and colon cancer cells (HCT15), and induces apoptosis by destroying ribosomal structures through direct binding to DNA.[7]

In 2020, Pei and coworkers[8] isolated four new cyclodepsipeptides trichodestruxins A–D (►**Fig. 1**) from the plant endophytic fungus *Trichoderma harzianum*, and elucidated their structures using 1D/2D nuclear magnetic resonance (NMR), high-resolution electrospray ionization mass spectrometry (HR-ESI-MS) spectroscopic analyses, the advanced Marfey's method, etc. In bioactivity assays, all cyclic peptides were cytotoxic to the tumor cell line A549 with IC_{50} values ranging from 8.8 to 17.5 μmol/L. However, trichodestruxin D was not as effective as trichodestruxins A–C in its antiproliferative ability against A549 cells.

Structural optimization of natural peptides is one of the effective methods to develop potential lead compounds, which can improve peptide stability while increasing activity. This includes reasonable chemical strategies based on methylation, acetylation, lipid substitution of acetyl groups, the introduction of functional groups, phosphorylation (especially tyrosine phosphorylation), cyclization, and so on.[9–12] Lokey's group reported more results regarding the effect of backbone *N*-methylation of the Sanguinamide A scaffold on biological activity. They found that the biological activity can be affected by the skeletal *N*-methylation, and can be greatly improved by the *N*-methylation at the Phe-NH site.[13] Jin's group synthesized a variety of methyl-modified and stereo-modified analogues of the marine cyclic peptide galaxamide with isoindolinone,[14] and demonstrated the benefit of monomethyl substitution in improving the biological activity of cyclic analogs with isoindolone fragments. Rekdal's group designed a series of derivatives by substituting amino acids of peptide L5 derived from the *N*-terminal α-helix region of bovine lactoferrin,[15] and disclosed a deep impact of the substitution of amino acids on the antitumor activity of the compound. The result revealed that the activity was enhanced by such modifications. Given the above, optimization of the natural peptides is one of the most effective ways to develop potential lead compounds. Therefore, we structurally modified trichodestruxin D in an attempt to improve its antiproliferative activity against tumor cells.

In this work, trichodestruxin D (**TD**-(*R*), as shown in ►**Fig. 1**) was used as the lead compound to explore a series of derivatives, which was composed of (*R*)-2-hydroxy-4-methylpentanoic acid ((*R*)-HMPA), a β-MePro unit, Val, *N*Me Val, *N*Me Ala, and β-Ala. Structure optimization of **TD**-(*R*) included the replacement of the unnatural amino acids with natural amino acids, the replacement of the ester group with the amide group, and the demethylation of the amide. In addition, (*R*)-HMPA was replaced with (*S*)-2-hydroxy-4-methylpentanoic acid to generate **TD**-(*S*) to assess the effect of configuration on the antitumor activity. The cytotoxicity of the derivatives against the lung carcinoma A549 cells was assessed and the structure and activity relationships were discussed. Our data suggested that **TD**-(*S*), **TD-1**, and **TD-2** displayed higher antiproliferative activity than the control (DMSO) group. However, **TD**-(*S*) and **TD-1** showed slightly decreased antiproliferative activity compared with **TD**-(*R*), demonstrating the importance of the configuration of HMPA and some residues in the backbone of **TD**-(*R*).

Results and Discussion

To investigate whether the configuration plays a role in the antitumor ability of **TD**-(*R*), (*R*)-2-hydroxy-4-methylpentanoic acid ((*R*)-HMPA) was replaced with (*S*)-2-hydroxy-4-methylpentanoic acid ((*S*)-HMPA), resulting in a compound named **TD**-(*S*) [(β-Ala-(*S*)-HMPA-Pro-Val-Val$_{\text{-Me}}$-Ala)]. The ester bond in **TD**-(*R*) was replaced with an amide bond to obtain **TD-2** [(β-Ala-Leu-Pro-Val-Val$_{\text{-Me}}$-Ala)] to study the effects of different functional groups and residues on the antitumor activity of the compound. *N*-methyl valine of **TD-2** was replaced by valine to give **TD-1** [(β-Ala-Leu-Pro-Val-Val-Ala)]. Leucine of **TD-2** was replaced with threonine to give **TD-3** [(β-Ala-Thr-Pro-Val-Val$_{\text{-Me}}$-Ala)], then changed β-Ala to *N*-Me-β-Ala to produce **TD-4** [(*β*-Ala$_{\text{-Me}}$-Leu-Pro-Val-Val$_{\text{-Me}}$-Ala)]. **TD-5** [(β-Ala-Leu-His-Val-Val-Ala)] was prepared by replacing the proline in **TD-1** with histidine, and **TD-6** [(β-Ala-Leu-His-Leu-Val-Ala)] was obtained by replacing the valine in **TD-5** with leucine. All the derivatives are shown in ►**Fig. 2** and the structures are confirmed by high-resolution mass spectra (HRMS).

TD-(*R*) and its derivatives were obtained by a solid-phase peptide synthesis (SPPS) to give linear peptides, head-to-tail cyclization in the liquid phase, and purified by reversed-phase preparative high-performance liquid chromatography (HPLC). Take **TD**-(*R*) for example: first, the building block, (*R*)-

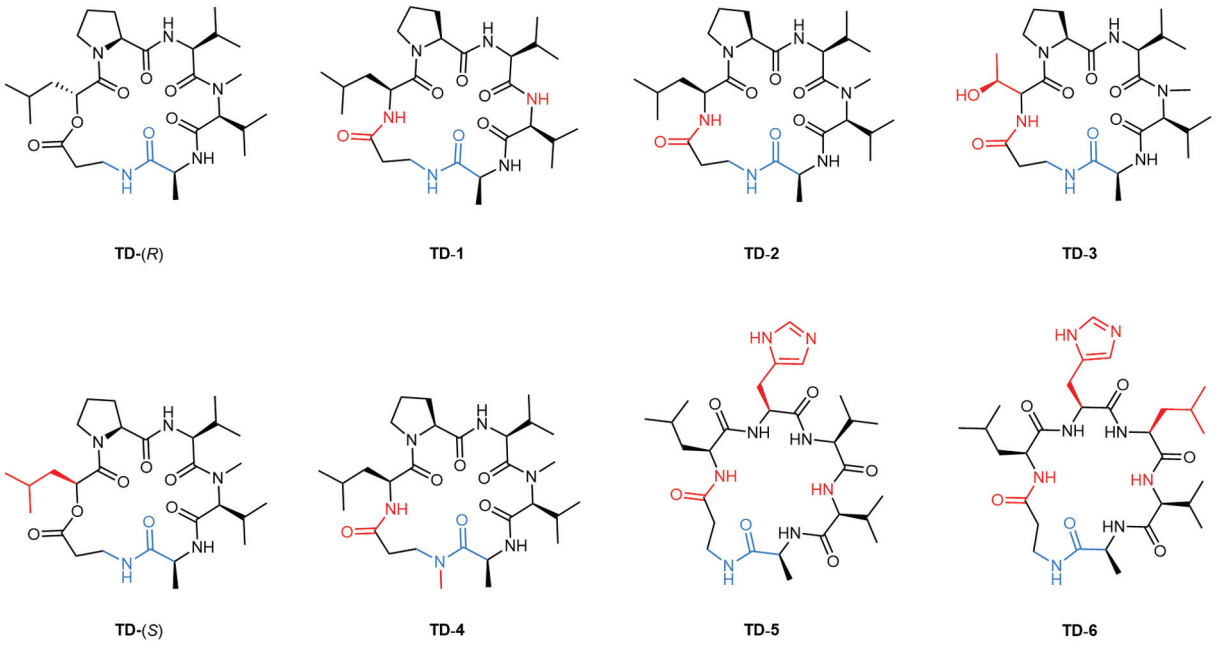

Fig. 2 Structures of trichodestruxin D and its derivatives.

2-((3-((*tert*-butoxycarbonyl)amino)propanoyl)oxy)-4-methylpentanoic acid (**5**), was synthesized (**Scheme 1**). The carboxyl group on (*R*)-HMPA (**2**) was protected by the benzyl group to generate compound **3**, then intermediate **3** was esterified with *N*-Boc-β-alanine to produce the intermediate **4**. Finally, the benzyl group was removed with palladium carbon to give the target compound **5**. (*S*)-2-((3-((*tert*-butoxycarbonyl)amino)propanoyl)oxy)-4-methylpentanoic acid (**9**) and **5** had the same chemical structure, yet opposite configuration. **9** can be obtained from (*S*)-HMPA (**6**) following the same synthesis route as compound **5**.

The linear peptide **12** was synthesized on 2-chlorotrityl chloride resin using the SPPS strategy (**Scheme 2**). The first amino acid was capped to the resin using *N,N'*-diisopropylethylamine (DIEA). Peptide couplings were performed using 1-hydroxybenzotriazole (HOBt) and *N,N'*-diisopropylcarbodiimide (DIC) in *N,N*-dimethylformamide (DMF). The Fmoc group was deprotected using 20% piperidine in DMF for 10 minutes. The linear peptide (**13**) was cleaved from the resin using 2,2,2-trifluoroethanol (TFE). The Boc group was then deprotected in the presence of trifluoroacetic acid (TFA) to obtain an intermediate (**14**). Finally, cyclic peptide **TD**-(*R*) was obtained by liquid-phase cyclization under the condition of 7-azabenzotriazol-1-yl-oxytris(pyrrolidino) phosphonium hexafluorophosphate (PyAOP), 1-hydroxy-7-azabenzotriazole (HOAt), and *N*-methylmorpholine (NMM).

CCK-8 cell viability assay was performed to evaluate the antitumor activity of the derivatives. The concentration was determined as 100 μmol/L based on our previous work.[16] The cytotoxicity of **TD-**(*S*) and **TD-1**, **2**, **3**, **4**, **5**, **6** on A549 cells is

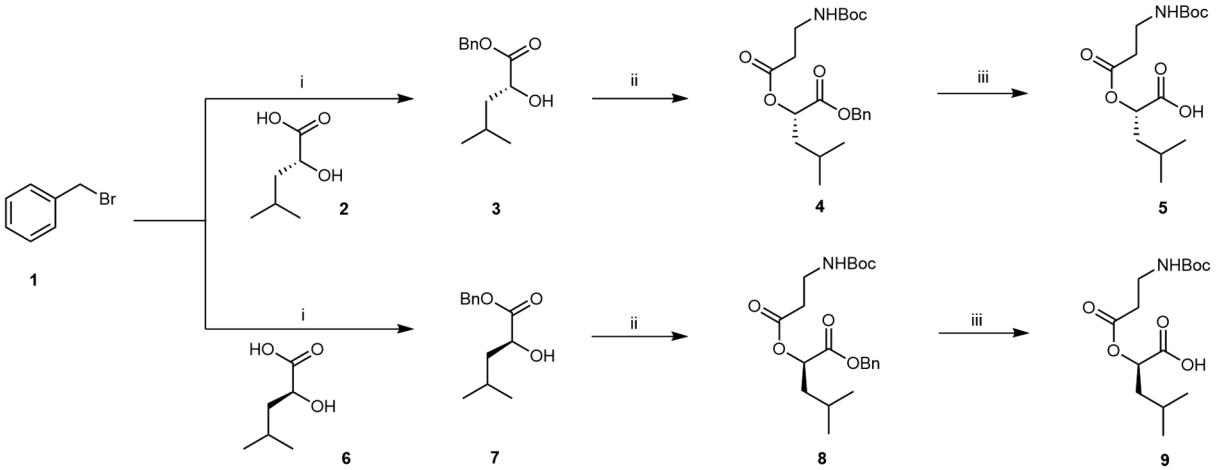

Scheme 1 Synthesis of (*R*)-2-((3-((*tert*-butoxycarbonyl)amino)propanoyl)oxy)-4-methylpentanoic acid (**5**) and (*S*)-2-((3-((*tert*-butoxycarbonyl)amino)propanoyl)oxy)-4-methylpentanoic acid (**9**). Reaction condition: (i) K_2CO_3, 75°C, 5 hours; (ii) *N*-Boc-*β*-alanine, DCC, DMAP, 25°C, 19 hours; (iii) palladium carbon, hydrogen protection, overnight. DCC, *N,N'*-dicyclohexylcarbodiimide; DMAP, 4-dimethylaminopyridine.

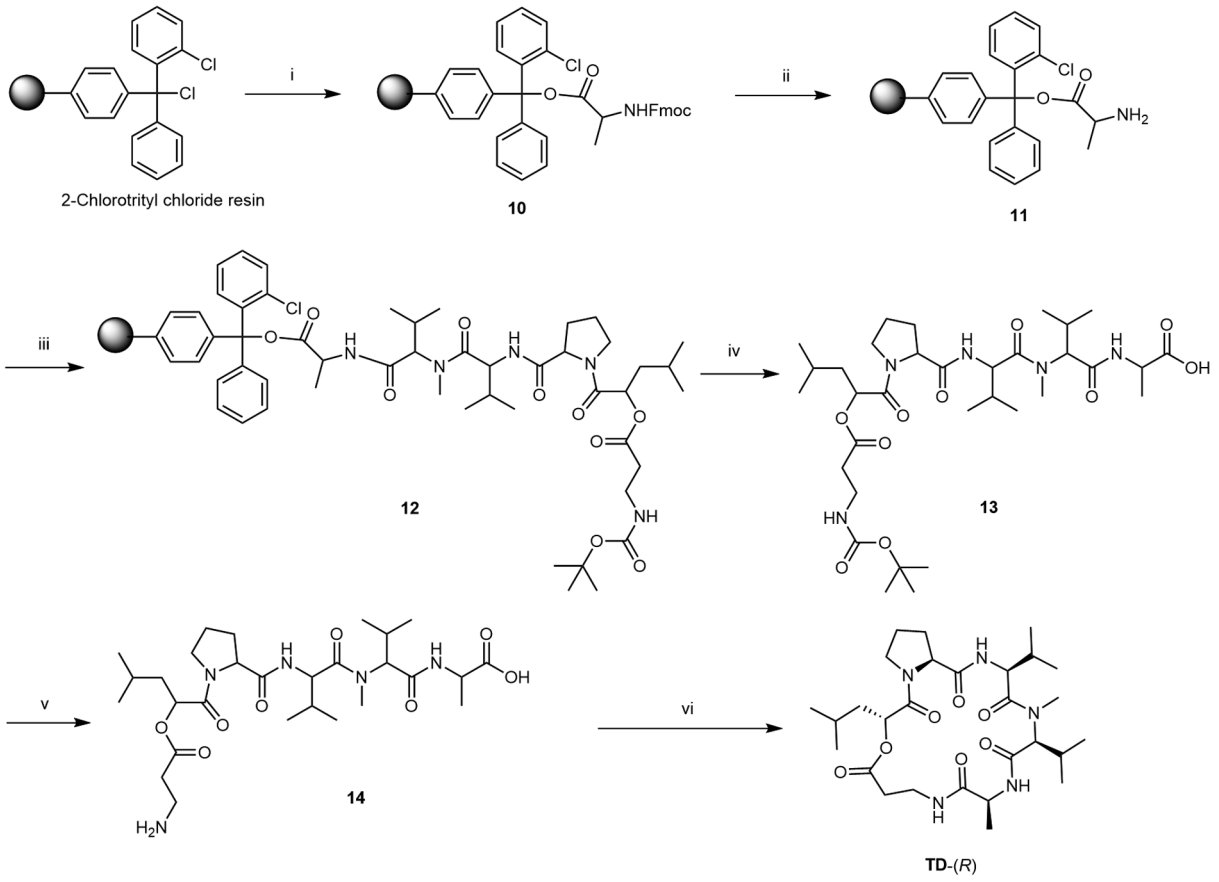

Scheme 2 Synthesis toward peptide **TD**-(*R*). Reaction condition: (i) Fmoc-Ala-OH, DIEA, DMF, 37°C, 2 hours; (ii) piperidine/DMF (1/4, v/v), 37°C, 5 minutes + 10 minutes; (iii) Fmoc-AA-OH, HOBt, DIC, DMF, 1 hour, 37°C; (iv) TFE, DCM, 37°C, 4 hours; (v) TFA, DCM, 37°C, 4 hours; (vi) PyAOP, HOAt, NMM, DMF, 37°C, 12 hours. DIC, *N,N'*-diisopropylcarbodiimide; DIEA, *N,N'*-diisopropylethylamine; HOBt, 1-hydroxybenzotriazole; HOAt, 1-hydroxy-7-azabenzotriazole; NMM, *N*-methylmorpholine; TFE, 2,2,2-trifluoroethanol.

shown in ►**Fig. 3A**. Our data suggested that **TD**-(*S*), **TD**-**1**, and **TD**-**2** showed much stronger inhibitory activity than the control (DMSO) group. Unfortunately, they did not show improved antitumor activity compared with **TD-**(*R*), even up to the concentration of 100 µmol/L. The result suggested the influence of the configuration of HMPA on the antitumor activity of **TD-**(*R*), with its antitumor activity being reduced when the configuration was *S*, and also suggested that the ester bond and the *N*-methyl on the scaffold of **TD**-(*R*) played an important role for the activity. **TD**-**3**, **4**, **5**, and **6** even did not show any inhibitory activity, indicating the importance of residues Leu, Pro, and Val for the activity of the compounds. The antitumor activity of **TD**-**3** was slightly decreased compared with **TD**-**2**, demonstrating that the Thr with polar but nonionized side chain was unfavorable. Pro residues have been proven helpful for the β-turn.[17] When the Pro of **TD**-**1** was substituted with His to generate **TD**-**5**, the cytotoxicity could decrease almost onefold, implying the importance of Pro in the activity. The cytotoxicity of **TD**-**4** was lower than that of **TD**-**2**, implying that *N*-methylation may not be favorable to the antitumor activity.

In some cases, malignant tumor cells can penetrate the body's barriers and invade the surrounding environment, destroying the surrounding tissues.[18,19] These cancer cells move to other parts of the body through the bloodstream or lymphatic system and invade other tissues of the body, growing and multiplying in the new organs to form metastatic tumors, which presents an additional challenge to clinical treatment.[20,21] In this regard, we evaluated the inhibitory activity of **TD**-(*R*)-derived peptides against the migration of A549 cells. As shown in ►**Fig. 3B**, **TD**-**3**, **TD**-**4**, and **TD**-**6** inhibited the migration of A549 cells at the dose of 100 µmol/L. In ►**Fig. 3C**, we could visually observe that **TD**-**3**, **TD**-**4**, and **TD**-**6** inhibited the migration of A549 cells better than **TD**-(*R*).

Conclusion

In the present study, a series of **TD-**(*R*) derivatives were designed and synthesized, and most of them displayed antitumor activity when compared with the DMSO control group. Cyclic hexapeptide **TD-**(*S*), **TD**-**1**, and **TD**-**2** showed much stronger antiproliferative activity in CCK-8 assays, but slightly decreased activity compared with **TD**-(*R*). It was also found that the configuration of **TD-**(*R*) affected the antiproliferative activity. When (*R*)-HMPA was replaced by (*S*)-HMPA, the antiproliferative activity of **TD-**(*S*) was decreased. The ester bond and *N*-methyl of Val also played an important role in the antitumor activity. It was concluded that most residues in **TD**-(*R*) including the configuration of HMPA are

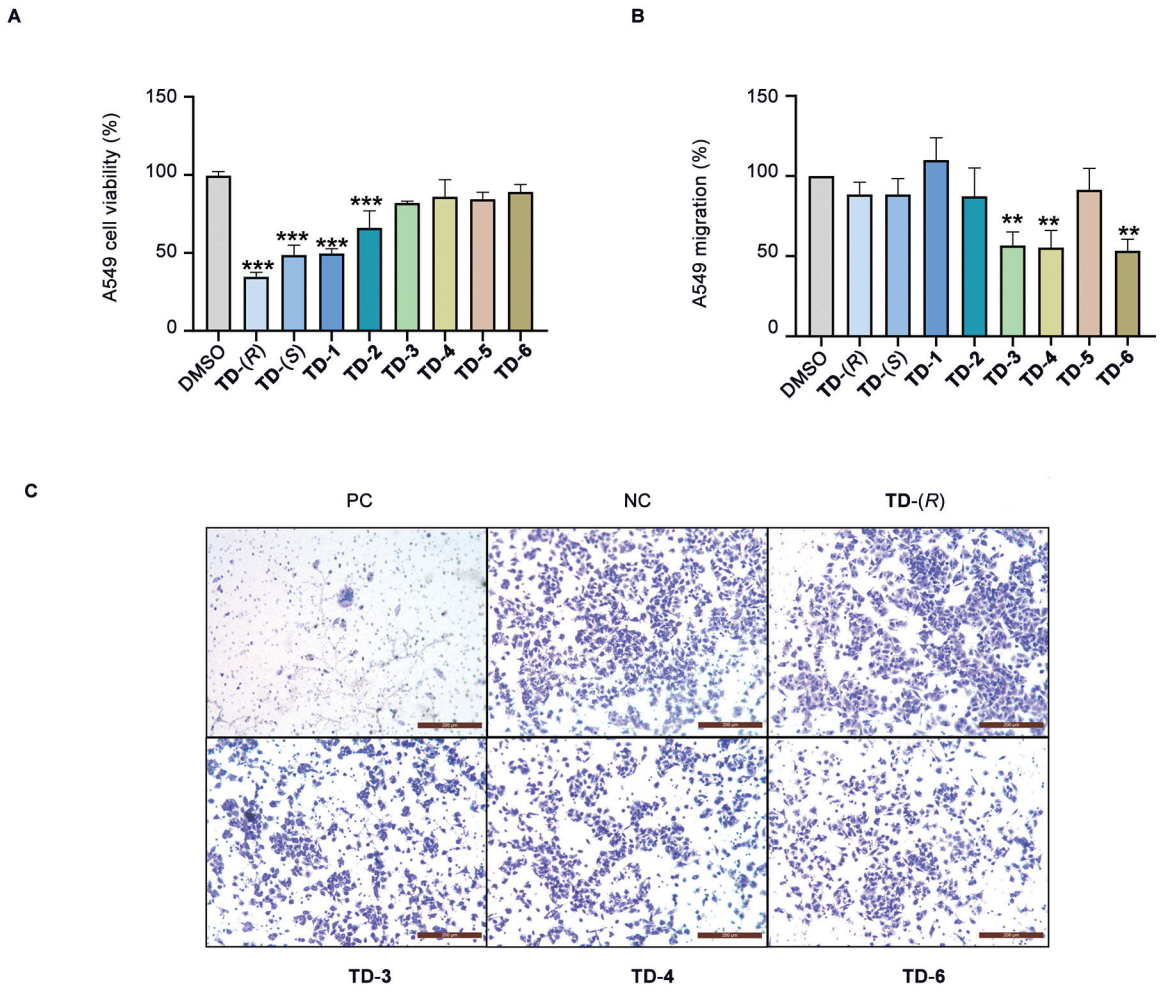

Fig. 3 **(A)** Effects of 100 μmol/L **TD**-(*R*) and **TD**-(*S*), and **TD-1**, **2**, **3**, **4**, **5, 6** on A549 cell viability. **(B)** Effects of 100 μmol/L **TD**-(*R*) and **TD**-(*S*), and **TD-1**, **2**, **3**, **4**, **5, 6** on the migration of A549 cells. **(C)** The migration of A549 cells was observed under a microscope when the cells were treated with 100 μmol/L **TD**-(*R*), **TD-3**, **TD-4**, and **TD-6**. Data were presented as mean ± standard error of the mean of at least three repeats. Data from **Fig. 3A** were analyzed using one-way ANOVA with GraphPad Prism software, and $p \leq 0.05$ was considered statistically significant. Data from **Fig. 3B** was obtained by cell counting with Image J software and one-way ANOVA with GraphPad Prism software for **Fig. 3C**. $p \leq 0.05$ was considered statistically significant. NC: negative controlled group (cells were treated with DMEM basal medium containing 1% DMSO and placed in the upper chamber). PC: positive controlled group (untreated cells with DMEM complete culture medium into the upper chamber). $^{**}p < 0.01$, $^{***}p < 0.001$ compared with the DMSO group. DMEM, Dulbecco's Modified Eagle's medium.

pivotal for the antitumor activity. However, **TD-3**, **TD-4**, and **TD-6** showed inhibitory activity in cancer cell migration assays and may be used as potent lead peptides for the treatment of tumor migration. The results provide a valuable reference for the development of peptide analogs to treat cancer in the future.

Experimental Section

Materials and General Procedures

Amino acids were purchased from CS Bio Ltd. (Shanghai, China). Wang resin and 2-chlorotriphenylmethyl chloride resin were provided by Tianjin Nankai Hecheng Science & Technology Co., Ltd. (Tianjin, China). All other reagents and solvents were supplied by Sinopharm Chemical Reagent Co. Ltd., Bide Pharmatech Ltd., and Shanghai Titan Scientific Co., Ltd. (Adamas-β) (Shanghai, China). Sterile Dulbecco's Modified Eagle's medium (DMEM), Trypsin-EDTA, fetal bovine serum (FBS), and penicillin-streptomycin used in biological assays were purchased from Gibco (Grand Island Biological Company, Grand Island, United States). The Cell Counting Kit-8 (CCK-8) was purchased from Beyotime Biotech Inc. (Shanghai, China). Phosphate-buffered saline (PBS), the Cell Culture Chamber (Falcon, 8.0 μm, PET membrane), and a 24-well migration plate were purchased from Shanghai Titan Scientific Co., Ltd. (Shanghai, China). A549 cells were purchased from the Cell Bank of the Chinese Academy of Sciences (Shanghai, China). The ^{1}H NMR and ^{13}C NMR spectra were determined using a Bruker AC-600P spectrometer (600 MHz for ^{1}H, and 151 MHz for ^{13}C). The solvent used for NMR spectra was chloroform-*d* with tetramethylsilane as internal standard. HRMS data were measured using an Agilent

Technologies 6538 UHD accurate-Mass Q-TOF MS spectrometer with electrospray ionization.

Reversed-Phase Analytical HPLC

Analytical HPLC was run on an Agilent 1260 Infinity LC instrument using an analytical column (ZORBAX Eclipse XDB 80 Å C18, 4.6 mm × 150 mm, 3.5 µm) with a flow rate of 1.0 mL/min and at room temperature. Analytical feeds were monitored at 214 and 254 nm. The mobile phases used for all separations were 0.1% TFA (v/v) in acetonitrile (solvent A) and 0.1% TFA (v/v) in water (solvent B). A linear gradient of 95% to 5% B was used for 40 minutes at room temperature.

Reversed-Phase Preparative HPLC

Semi-preparative HPLC was run on a Pre-HPLC Agilent 1100 Series (United States) instrument using a semi-preparative column (CST Daiso Prep C18; 30 mm × 250 mm, 10 µm particle size) The flow rate was 30 mL/min. Solution A was acetonitrile containing 0.1% TFA. Solution B was H_2O containing 0.1% TFA. A linear gradient of 95% to 95% B was used for over 5 minutes, and a linear gradient of 95% to 15% B is then applied over 55 minutes at room temperature. All peptides had a purity of at least 95%.

Synthesis of (*R*)-2-((3-((*tert*-butoxycarbonyl)amino) propanoyl)oxy)-4-methylpentanoic Acid (Compound 5)

(*R*)-HMPA (2.64 g, 20 mmol, 1 equiv.) was dissolved in acetone (100 mL), then K_2CO_3 (5.52 g, 40 mmol, 2 equiv.) and benzyl bromide (5.13 g, 30 mmol, 1.5 equiv.) were added. The reaction was stirred at 75°C for 5 hours. The crude product (**3**) was purified on a silica gel column (petroleum ether/ethyl acetate, 20/1, v/v). Benzyl (*R*)-2-hydroxy-4-methylpentanoate (**3**) (2.22 g, 10 mmol, 1 equiv.) and *N*-Boc-β-alanine (2.84 g, 15 mmol, 1.5 equiv.) were dissolved in dichloromethane (DCM; 100 mL), then 4-dimethylaminopyridine (DMAP; 0.61 g, 0.5 mmol, 0.05 equiv.) and *N*,*N*'-dicyclohexylcarbodiimide (DCC; 3.09 g, 15 mmol, 1.5 equiv.) were added to the solution at 0°C. After 30 minutes, the solution was stirred at 25°C for 19 hours. The solution was filtered, concentrated, and dissolved in Et_2O, then extracted with 1 mmol/L cold HCl, saturated $NaHCO_3$ solution, and NaCl solution, respectively. The organic layer was dried with anhydrous Na_2SO_4, then filtered and concentrated. The crude product (**4**) was purified on a silica gel column (petroleum ether/ethyl acetate, 8/1, v/v). The compound **4** (3.93 g, 10 mmol, 1 equiv.) was dissolved in methanol, and then palladium carbon (0.11 g, 1 mmol, 0.1 equiv.) was added under hydrogen protection. The reaction was stirred at 25° C for 6 hours, then filtered and concentrated to give compound **5**. Yield: 67%, clear and colorless oil, purity: 96.4%. ^{1}H NMR (600 MHz, $CDCl_3$) δ 8.40 (s, 1H), 5.26 (s, 1H), 5.07 (dd, J = 9.0, 3.6 Hz, 1H), 3.39 (d, J = 29.4 Hz, 2H), 2.63–2.53 (m, 2H), 1.83–1.72 (m, 2H), 1.71–1.64 (m, 1H), 1.43 (d, J = 24.6 Hz, 9H), 0.94 (d, J = 6.6 Hz, 3H), 0.91 (d, J = 6.6 Hz, 3H). ^{13}C NMR (151 MHz, $CDCl_3$) δ 174.97, 172.13, 156.15, 79.66, 70.87, 39.54, 36.25, 34.52, 28.33, 24.65, 22.96, 21.48. HRMS m/z calcd. for $C_{14}H_{25}NO_6Na^+$ $[M+Na]^+$ 326.1575, found: 326.1573.

Synthesis of (*S*)-2-((3-((*tert*-butoxycarbonyl)amino) propanoyl)oxy)-4-methylpentanoic Acid (Compound 9)

Compound **9** was synthesized in the same way as compound **5**, except that using (*S*)-HMPA, instead of (*S*)-HMPA, as the starting material. Compound **9**, yield 53%, clear and colorless oil, purity: 93.5%. ^{1}H NMR (600 MHz, $CDCl_3$) δ 7.72 (s, 1H), 5.23 (s, 1H), 5.08 (dd, J = 9.6, 3.6 Hz, 1H), 3.40 (d, J = 27 Hz, 2H), 2.64–2.53 (m, 2H), 1.86–1.73 (m, 2H), 1.73–1.65 (m, 1H), 1.44 (d, J = 22.8 Hz, 9H), 0.95 (d, J = 6.6 Hz, 3H), 0.92 (d, J = 6 Hz, 3H). ^{13}C NMR (151 MHz, $CDCl_3$) δ 175.11, 172.12, 156.11, 79.65, 70.86, 39.54, 36.25, 34.55, 28.34, 24.66, 22.97, 21.49. HRMS m/z calc. for $C_{14}H_{25}NO_6Na^+$ $[M+Na]^+$ 326.1575, found: 326.1569.

Synthesis of TD-(*R*) and TD-(*S*)

The linear peptide was synthesized on 2-chlorotrityl chloride resin (100–200 mesh, loading amount 1.12 mmol/g, 0.89 g, 1 mmol) via the strategy of SPPS. Peptide couplings were performed using HOBt (0.41 g, 3 mmol, 3 equiv.), DIC (0.58 g, 4.5 mmol, 4.5 equiv.), DMF (25 mL), and shaken for 2 hours at 25°C. Following the completion of each stage of the reaction, the solvent was drained and the resin was washed with DCM and DMF. The Fmoc group was deprotected using 20% piperidine in DMF (20 mL) at 25°C for 15 minutes. After the linear peptide **12** was assembled, it was cleaved from the resin using a mixture of TFE and DCM (1:3, v/v, 30 mL) at 25°C for 4 hours to produce Boc-protected peptide **13**. After intermediate **13** was purified by semi-preparative reverse-phase HPLC, it was dissolved in the solution of TFA and DCM (1:3, v/v, 30 mL) and stirred at 25°C for 4 hours to give **14**. Then, the linear peptide **14** (0.2 g, 0.34 mmol, 1 equiv.) was dissolved in DCM (200 mL) with the concentration of 1 mg/mL, and then PyAOP (0.89 g, 1.7 mmol, 5 equiv.), HOAt (0.23 g, 1.7 mmol, 5 equiv.), and NMM (0.4 g, 3.4 mmol, 10 equiv.) were added and stirred at 25°C for 12 hours. The solvent was evaporated in vacuo to give the crude cyclic peptide **TD**-(*R*), which was purified by semi-preparative RP-HPLC. The purity and the structure of **TD**-(*R*) were confirmed by analytical HPLC and HRMS. **TD**-(*R*) was lyophilized into a white powder with a yield of 13% and a purity of 96.9%. HRMS m/z calcd. for $C_{28}H_{48}N_5O_7^+$ $[M+H]^+$ 566.3549, found: 566.3547.

TD-(*S*) was synthesized in the same procedure with a yield of 10% and a purity of 98.6%, as a white powder. HRMS m/z calcd. for $C_{28}H_{48}N_5O_7^+$ $[M+H]^+$ 566.3549, found: 566.3584.

Cell Culture and Treatment

A549 cells were cultured in DMEM (Gibco) supplemented with 1% penicillin/streptomycin (EMD Millipore) and 10% FBS (Gibco). Place the cells in a humidified constant temperature incubator with 5% CO_2 and maintain at 37°C.

CCK-8 Cell Viability assay

A549 cells were seeded at 5×10^3 per well in a clear 96-well plate and incubated at 37°C in 5% CO_2 overnight. The groups were divided into a control group (cells treated with DMEM basal medium containing 1% DMSO) and drug administration groups. The cells in drug administration groups were treated with each cyclic peptide (100 µmol/L) in triplicate for

72 hours. The supernatant was removed and prepared reagent (CCK-8 reagent solution and serum-free DMEM medium were mixed in a volume of 1:10) was added to each well (100 µL/well). Then, A549 cells were incubated at 37°C in 5% CO_2 for 30 minutes. Absorbance values were measured on a SpectraMax M5 microplate reader at 450 nm.

Cell Migration Assay

A549 cells were seeded at 4×10^4 cells/well into the upper chamber containing 300 µL of DMEM basal medium, and 700 µL of complete medium containing serum was added to the lower chamber of a 24-well transfer plate. The groups were divided into negative control (cells were treated with DMEM basal medium containing 1% DMSO and placed in the upper chamber), positive control (untreated cells with DMEM complete culture medium containing 10% FBS into the upper chamber), and drug administration groups. The cyclic peptide (100 µmol/L) was added to the upper chamber, and incubated in a thermostatic incubator at 37°C in 5% CO_2 for 24 hours. Cells in the upper chamber were gently wiped off with a sterile cotton swab and fixed with 10% formaldehyde solution for 30 minutes. The upper chambers were washed with PBS (5 minutes × 3), then the fixed cells were stained with 5% crystal violet solution for 20 minutes, and washed again with PBS (5 minutes × 3). Finally, the cells were observed under a microscope and photographed, and cell counting was determined by Image J software. Each experiment was performed with three replicates.

Supporting Information

Full experimental detail and synthesis route for the peptide **TD-1**, **2**, **3**, **4**, **5**, and **6** (**Schemes S1–S3**), the migration of A549 cells observed under a microscope when the cells were treated with 100 µmol/L **TD-**(*S*), **TD-1**, **TD-2**, and **TD-5** (►**Fig. S1**); the ^1H, ^{13}C NMR, HRMS spectra, and HPLC of compound **5**, **9**, as well as HRMS spectra and HPLC of the peptide **TD-**(*R*), **TD-**(*S*), **TD-1**, **2**, **3**, **4**, **5**, **6** (►**Fig. S2–S15**) can be found in the "Supporting Information" section of this article's webpage.

Conflict of Interest

None declared.

References

1 Xia L, Wu Y, Ma JI, Yang J, Zhang F. The antibacterial peptide from *Bombyx mori* cecropinXJ induced growth arrest and apoptosis in human hepatocellular carcinoma cells. Oncol Lett 2016;12(01): 57–62

2 Ellerby HM, Arap W, Ellerby LM, et al. Anti-cancer activity of targeted pro-apoptotic peptides. Nat Med 1999;5(09):1032–1038

3 Liao N, Sun L, Chen J, Zhong J, Zhang Y, Zhang R. A novel polysaccharide conjugate from Bullacta exarata Induces G1-phase arrest and apoptosis in human hepatocellular carcinoma HepG2 cells. Molecules 2017;22(03):384

4 He R, Liu M, Zou Z, et al. Anti-inflammatory activity of peptides derived from millet bran *in vitro* and *in vivo*. Food Funct 2022;13 (04):1881–1889

5 Zhang Z, Jiang S, Tian H, et al. Ethyl acetate fraction from Nymphaea hybrida Peck modulates inflammatory responses in LPS-stimulated RAW 264.7 cells and acute inflammation murine models. J Ethnopharmacol 2021;269:113698

6 Gao C, Sun R, Xie YR, et al. The soy-derived peptide Vglycin inhibits the growth of colon cancer cells *in vitro* and *in vivo*. Exp Biol Med (Maywood) 2017;242(10):1034–1043

7 Mandal SM, Migliolo L, Das S, Mandal M, Franco OL, Hazra TK. Identification and characterization of a bactericidal and proapoptotic peptide from Cycas revoluta seeds with DNA binding properties. J Cell Biochem 2012;113(01):184–193

8 Liu Z, Sun Y, Tang M, et al. Trichodestruxins A-D: cytotoxic cyclodepsipeptides from the endophytic fungus *Trichoderma harzianum*. J Nat Prod 2020;83(12):3635–3641

9 Chiangjong W, Chutipongtanate S, Hongeng S. Anticancer peptide: physicochemical property, functional aspect and trend in clinical application (Review). Int J Oncol 2020;57(03):678–696

10 Peng S, Barba-Bon A, Pan YC, Nau WM, Guo DS, Hennig A. Phosphorylation-responsive membrane transport of peptides. Angew Chem Int Ed Engl 2017;56(49):15742–15745

11 Khayat E, Klimov DK, Smith AK. Phosphorylation promotes Aβ25-35 peptide aggregation within the DMPC bilayer. ACS Chem Neurosci 2020;11(20):3430–3441

12 Wallace RJ. Acetylation of peptides inhibits their degradation by rumen micro-organisms. Br J Nutr 1992;68(02):365–372

13 Bockus AT, Schwochert JA, Pye CR, et al. Going out on a limb: delineating the effects of β-branching, N-methylation, and side chain size on the passive permeability, solubility, and flexibility of sanguinamide A analogues. J Med Chem 2015;58(18):7409–7418

14 Xiao S, Wang Z, Zhang H, et al. Photoinduced synthesis of methylated marine cyclopeptide galaxamide analogs with isoindolinone as anticancer agents. Mar Drugs 2022;20(06):379

15 Yang N, Lejon T, Rekdal O. Antitumour activity and specificity as a function of substitutions in the lipophilic sector of helical lactoferrin-derived peptide. J Pept Sci 2003;9(05):300–311

16 Li A, Zou J, Zhuo X, et al. Rational Optimizations of the Marine-Derived Peptide Sungsanpin as Novel Inhibitors of Cell Invasion. Chem Biodivers 2023;20(02):e202201221

17 Che Y, Marshall GR. Privileged scaffolds targeting reverse-turn and helix recognition. Expert Opin Ther Targets 2008;12(01):101–114

18 Kimura Y, Negishi H, Matsuda A, et al. Novel chemical compound SINCRO with dual function in STING-type I interferon and tumor cell death pathways. Cancer Sci 2018;109(09):2687–2696

19 Friedl P, Locker J, Sahai E, Segall JE. Classifying collective cancer cell invasion. Nat Cell Biol 2012;14(08):777–783

20 Deborde S, Omelchenko T, Lyubchik A, et al. Schwann cells induce cancer cell dispersion and invasion. J Clin Invest 2016;126(04): 1538–1554

21 Novikov NM, Zolotaryova SY, Gautreau AM, Denisov EV. Mutational drivers of cancer cell migration and invasion. Br J Cancer 2021;124(01):102–114

